Copyright © 2014 by American Scientific Publishers
All rights reserved.
Printed in the United States of America

Journal of Nanofluids
Vol. 3, pp. 51–59, 2014
(www.aspbs.com/jon)

Effects of Particle Migration on Nanofluid Forced Convection Heat Transfer in a Local Thermal Non-Equilibrium Porous Channel

T. Armaghani[1,*], M. J. Maghrebi[2], Ali J. Chamkha[3], and M. Nazari[1]

[1]*Department of Mechanical Engineering, Shahrood University, Shahrood, 3619995161, Iran*
[2]*Department of Mechanical Engineering, Ferdowsi University of Mashhad, Mashhad, 9177948974, Iran*
[3]*Manufacturing Engineering Department, The Public Authority for Applied Education and Training, Shuweikh 70654, Kuwait*

This paper is concerned with the effects of flow and migration of nanoparticles on heat transfer in a straight channel occupied with a porous medium. Investigation of forced convective heat transfer of nanofluids in a porous channel has not been considered completely in the literature and this challenge is generally considered to be an open research topic that may require more study. The fully-developed flow and steady Darcy-Brinkman equation is employed in the porous channel. The local thermal non-equilibrium model is assumed between the pure fluid, solid and the nanoparticle phases. It is assumed that the nanoparticles are distributed non-uniformly inside the channel. As a result, the volume fraction distribution equation is also coupled with governing equations. The effects of Lewis number, Schmidt number and modified diffusivity ratio (N_{bt}) on the heat transfer are completely studied. The results show that the non-dimensional heat flux absorbed by fluid is decreased when the Lewis number is increased. This behaviour can also be observed in the heat flux absorbed by the particles and the solid. The effects of Scmith number, Lewis number and N_{bt} on the volume fraction distribution and the heat flux are also studied numerically. The results indicate that when the Schmith number is increased the particle distribution tend to the entrance distribution. The effect of N_{bt} on the heat flux and the volume fraction is studied and discussed as well.

Delivered by Publishing Technology to: Guest User
IP: 31.214.93.254 On: Thu, 12 Dec 2013 21:46:38
Copyright: American Scientific Publishers

KEYWORDS: Heat Flux, Particle Migration, Porous Channel, Volume Fraction Distribution.

ARTICLE

1. INTRODUCTION

Nanofluid, a name conceived by Choi[1] at Argonne National laboratory, are fluids consisting of solid nanoparticles with size less than 100 nm suspended with solid volume fraction typically less than 4%. A nanofluid can enhance heat transfer performance compared to pure liquids. Nanofluids can be used to improve thermal management system in many engineering application such as transportation, micromechanics and instrument, HVAC system and cooling devices. Recently, many investigators studied nanofluid convective heat transfer in different geometry both numerically and experimentally.[3–6] For numerical simulation, two approaches have been adopted in the literature to investigate the heat transfer characteristics of nanofluids, the single-phase model and the two-phase model. Another approach is to adopt the Boltzmann theory.[7] In the single-phase model, a uniform volume fraction distribution is assumed for nanofluids. In other words, the viscosity and thermal conductivity of nanofluids are formulated by volume fraction and nanoparticle size then continuity, momentum and energy equations are solved for nanofluids. In the two-phase model, the volume fraction distribution equation is added to other conservation equations. Many authors used the single- and two-phase models for investigating the flow and heat transfer of nanofluids.[8–10] Tayebi et al.[11] studied the effect of sinusoidal thermal boundary condition on natural convection in a cavity filled with Cu-Water nanofluid numerically. They assumed the single-phase approach for a nanofluid. The results showed that the uniform temperature at the bottom wall gave a higher Nusselt number compared to the sinusoidal varying temperature case for $\varphi = 0$, 0.05 and 0.1 for bottom wall. For a given Rayleigh number, an increase of the volume fraction of nanoparticles caused an increase in the mean Nusselt number, but this increment was high for the case of constant temperature.

*Author to whom correspondence should be addressed.
Email: taherarmaghani@yahoo.com
Received: 21 June 2013
Accepted: 16 July 2013

Buongiorno[12] introduced seven slip mechanisms between nanoparticles and the base fluid. He showed that the Brownian motion (movement of nanoparticles from high concentration site) and thermophoresis (movement of nanoparticles from the high temperature site to the low temperature site) have significant effect in the laminar forced convection of nanofluids. Based on this finding, he developed non-homogeneous two-component equations in nanofluids. Heyhat and Kowsary[13] used Buongiorno's model for investigating the effect of particles migration on flow and convective heat transfer of nanofluids flowing through a circular pipe. Their results show that the non-uniform distribution leads to a higher heat transfer coefficient while the wall shear stress is decreased. Therefore, the particle migration can play an important role in improvement of the heat transfer coefficient in convective heat transfer in nanofluids.

In recent papers, written by Kuznetsov and Nield,[14–16] the Buongiorno's model was applied to the Horton-Rogers-Lapwood problem (the onset of convention in a horizontal layer of a porous medium uniformly heated from below). Both Brownian motion and thermophoresis give rise to cross-diffusion terms that are in some way analogous to the familiar Sort and Dufour cross-diffusion terms that arise with a binary fluid. Nield and Kuznetsov[17] introduced an analytical treatment of double-diffusive natural convection boundary layer flow in a porous medium saturated by nanofluid. They used the Buongiorno's equation for modeling the nanofluid and Darcy model for porous medium. The results showed a decrease in the reduced Nusselt number associated with an increase in the thickness of the thermal boundary layer, an increase in the Brownian motion parameter, buoyancy ratio, thermophoresis parameter, modified Dufour parameter and a decrease in the regular buoyancy ratio. The analytical treatment of double-diffusive natural convection boundary layer flow of a nanofluid past a vertical plate was also studied by Kuznetsov and Nield.[18] Hajipour and Dehkordi[19] used Buongiorno's model for an analytical investigation of nanofluid heat transfer in a parallel-plate vertical partially filled with a porous medium. The predicted results clearly indicated that the presence of nanoparticles in the base fluid enhanced the heat transfer process significantly.

Delivered by Publishing Technology to: Guest User
IP: 31.214.93.254 On: Thu, 12 Dec 2013 21:46:38
Copyright: American Scientific Publishers

Prabhat et al.[20] investigated convective heat transfer enhancement in a nanofluid. They compared the 46 published papers in convective heat transfer of a nanofluid with the theoretical correlations of Dittus-Boelter's for turbulent flow and Shah's for laminar flow. All of the papers examined and 12 papers claimed significant deviations from the above correlations. They judged the deviation anomalous. The authors suggested more detailed study of physical mechanisms of a nanofluid. Two recent papers focused on this idea.[21,22] The new model for a nanofluid conductivity was introduced by Li et al.[21] The model included two different contribution of a nanofluid. The first was the combined thermophysical properties of the suspension resulting from the addition of the nanoparticles to the base fluid, and the second was the effect of the micro convection due to nanoparticle's Brownian motion. The new model showed excellent agreement when compared with existing experimental data.

Yu et al.[22] focused on the effective thermal conductivity models for carbon nanotube-based nanofluids. The results showed that most of the experimental data fell within the lower bound set by the linear decrease distribution model and the upper bound set by the linear increase distribution model and that most of the experimental data could be predicted by the combination of the uniform distribution model and the linear increase distribution model.

Convective instability in a thin layer of a magnetic nanofluid was studied by Mahajan et al.[23] The results showed that the increase in the magnetic field and the particle concentration near the lower boundary tended to stabilize the system. The magnetic mechanism predominated over the buoyancy mechanism in thin fluid layers of about 1 mm only. The increase in the particle concentration near lower (upper) wall could enhance (reduce) the thermal Rayleigh number. Gorla and Kumari[24] investigated the mixed convection flow of a non-Newtonian nanofluid over a non-linearly stretching sheet. Their results showed the effect of the thermophoresis number, as well as the Brownian motion number on the velocity, angular velocity, temperature and concentration profiles. As the thermophoresis number increased, the velocity, temperature and the concentration within the boundary layer increased. Also, as the Brownian motion number increased, the temperature increased whereas the velocity and concentration within the boundary layer decreased.

The effects of particle migration on forced convective heat transfer of nanofluid in a porous medium at thermal equilibrium were investigated by Maghrebi et al.[25] They showed that the particles migration had a significant role in heat transfer. The results showed that the local Nusselt number was decreased when the Lewis number was increased. It was observed that as the Schmidt number was increased, the wall temperature gradient was decreased and as a consequence, the local Nusselt number was decreased. The effects of the Lewis number, Schmidt number and the modified diffusivity ratio on the volume fraction distribution were also studied and discussed.

2. GOVERNING EQUATIONS

The forced convection heat transfer in a two-dimensional channel is investigated numerically by solving the mathematical formulations introduced in this section. The geometry of the present problem is a 2D channel totally occupied with a porous medium as shown in Figure 1. The Cartesian coordinate is used for this geometry. The height of the channel is equal to 2H.

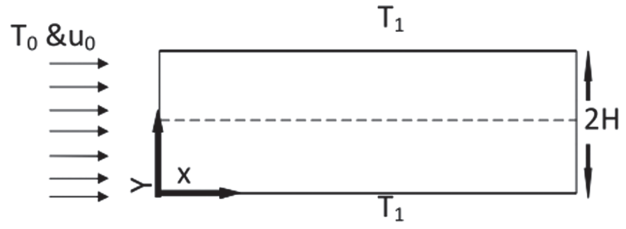

Fig. 1. Geometry of problem and coordinate system.

The nanofluid, treated as a two-component mixture, is flown in the channel as discussed by Buongiorno.[12]

The dimensionless fully developed and steady Darcy-Brinkman (DB) equation can be used for fluid flow in porous medium. The Brinkman term in this equation represents the viscous effects and makes it possible to impose a no-slip boundary condition at the impermeable wall.

$$\nabla^{*2}u^* - \frac{u^*}{\mathrm{Da}} - \frac{1}{\mathrm{Da}}\frac{1}{H^2}\frac{dP^*}{dx^*} = 0 \tag{1}$$

A three-temperature model for nanofluid heat transfer under local thermal non-equilibrium porous media was introduced by Kuznetsov and Nield.[15] The dimensionless energy equations for the fluid, particles and the solid are given as follows, respectively.

Delivered by Publishing Technology to: Guest User
IP: 31.214.93.254 On: Thu, 12 Dec 2013 21:46:38
Copyright: American Scientific Publishers

$$\frac{\partial T_f^*}{\partial t^*} + u^*\frac{\partial T_f^*}{\partial x^*} = \frac{1}{\mathrm{RePr}}\left[\nabla^{*2}T_f^* + \frac{\tau}{\mathrm{Le}}(\nabla^*\varphi^*\cdot\nabla^*T^*) + \frac{\tau}{\mathrm{Le}N_{\mathrm{bt}}} \times (\nabla^*T_f^*\cdot\nabla^*T_f^*) + N_{hp}(T_p^* - T_f^*) + N_{hs}(T_s^* - T_f^*)\right] \tag{2}$$

$$\frac{\partial T_p^*}{\partial t^*} + \frac{1}{\varepsilon}u^*\cdot\nabla^*T_p^* = \frac{1}{\mathrm{RePr}}[\varepsilon_p\nabla^{*2}T_p^* + \gamma_p N_{hp}(T_f^* - T_p^*)] \tag{3}$$

$$\frac{\partial T_s^*}{\partial t^*} = \frac{1}{\mathrm{RePr}}[\varepsilon_s\nabla^{*2}T_s^* + \gamma_s N_{hs}(T_f^* - T_s^*)] \tag{4}$$

The dimensionless volume fraction distribution is given as follow

$$\frac{\partial\varphi^*}{\partial t^*} + \frac{1}{\varepsilon}u^*\cdot\frac{\partial\varphi^*}{\partial x^*} = \frac{1}{\mathrm{ReSc}}\left[\nabla^2\varphi^* + \frac{1}{N_{\mathrm{bt}}}(\nabla^2T_f^*)\right] \tag{5}$$

The dimensionless parameters can be written as:

$$u^* = \frac{u}{u_0}, \quad (x^*, y^*) = \frac{(x,y)}{H}, \quad \varphi^* = \frac{\varphi}{\varphi_0}$$

$$t^* = \frac{t\,u_0}{H}T_f^* = \frac{T_f - T_0}{T_1 - T_0}, \quad T_s^* = \frac{T_s - T_0}{T_1 - T_0}$$

$$T_P^* = \frac{T_P - T_0}{T_1 - T_0}p^* = \frac{P\mu u_0}{KH}, \quad \nabla^* = \frac{\partial}{\partial(x^*, y^*)}$$

where u_0 is the average velocity in the channel, T_0 and φ_0 are the temperature and the particle volume fraction at the channel inlet, T_1 is the wall temperature and H is a characteristic length of the channel.

Nield et al.[26] indicated that the viscous dissipation term was directly proportional to Brinkman number defined as $\mu U^2H/k\Delta TK$ with k, ΔT and K as conductivity, temperature difference and permeability. This non-dimensional parameter was first defined in Eq. (15) of Nield et al.[26] In the present study, the order of magnitude of the aforementioned term is negligible in comparing with other terms of the energy equation. In other words, as the temperature difference between the wall and nanofluids increased, the viscous dissipation can be ignored. This assumption is often made in heat transfer problem in which the temperature (or heat flux) at the surface is the dominant energy source of the system.

The dimensionless parameters are defined as follows.

$$\mathrm{Sc} = \frac{\mu}{\rho D_B}, \quad \mathrm{Le} = \frac{\alpha_f}{D_B\varphi_0}, \quad \mathrm{Re} = \frac{u_0H}{\nu}, \quad \mathrm{Pr} = \frac{\nu}{\alpha_f}$$

$$\alpha_f = \frac{k_f}{(\rho c)_f}, \quad \tau = \frac{\varepsilon(\rho c)_p}{(\rho c)_f}, \quad N_{hp} = \frac{H^2h_{fp}}{\varepsilon(1-\varphi_0)k_f}$$

$$N_{hs} = \frac{H^2h_{fs}}{\varepsilon(1-\varphi_0)k_f}, \quad \gamma_p = \frac{(1-\varphi_0)}{\varphi_0}\frac{(\rho c)_f}{(\rho c)_p}$$

$$\gamma_s = \frac{\varepsilon(1-\varphi_0)}{(1-\varepsilon)}\frac{(\rho c)_f}{(\rho c)_s}, \quad \varepsilon_p = \frac{k_p}{k_f}\frac{(\rho c)_f}{(\rho c)_p}, \quad \varepsilon_s = \frac{k_s}{k_f}\frac{(\rho c)_f}{(\rho c)_s}$$

$$\mathrm{Da} = \frac{K}{H^2\varepsilon}N_{\mathrm{bt}} = \frac{D_B\varphi_0T_1}{D_T\Delta T}$$

where Da, Δ, Re, Sc, Pr are the Darcy number, inertia parameter, Reynolds number, Schmidt number and the Prantdl number, respectively. The parameter Le is the nanofluid's Lewis number. τ is the modified particle-density increment and N_{bt} is a modified diffusivity ratio. This parameter can be expressed as the ratio of Brownian diffusion to the thermophoresis diffusion. The N_{hp} and N_{hs} are the interface heat transfer parameters. Vadasz[27] called this type of parameter as the Nield number, citing Nield,[28] while elsewhere in the recent literature, it has been called as the Sparrow number. Because two other parameters have been called Sparrow numbers (an internal heating parameter and a radiation resistance parameter) in the heat transfer literature, we will follow Vadasz and adopt the terminology Nield number for the fluid/particle interface and Nield number for the fluid/solid-matrix interface, respectively. γ_p and γ_s are the modified thermal capacity ratio. ε_p and ε_s are the modified thermal diffusivity ratios for particle and solid respectively.

Amiri et al.[29] introduced the boundary condition model for considering heat flux in a two-temperature equation (local thermal non-equilibrium porous media with pure fluid), we improved that to local thermal non-equilibrium problem in the presence nanoparticles. The heat flux

ARTICLE

absorbed by the fluid, particles and the solid phases (at a representative elementary volume), are related together according to the following equation.

$$q'' = q''_f + q''_p + q''_s = \varepsilon(1-\varphi)k_f\left(\frac{\partial T_f}{\partial y}\right)_{\text{wall}} + \varepsilon(\varphi)k_p\left(\frac{\partial T_p}{\partial y}\right)_{\text{wall}} + (1-\varepsilon)k_s\left(\frac{\partial T_s}{\partial y}\right)_{\text{wall}} \quad (6)$$

The non-dimensional heat flux is:

$$Q^* = \frac{q''}{k_f((T_1 - T_0)/H)} \quad (7)$$

Then, the non-dimensional heat flux absorbed by fluid, particle and solid phases are introduced:

$$Q^*_f = \varepsilon(1-\varphi^*\varphi_0)\left(\frac{\partial T^*_f}{\partial y^*}\right)_{\text{wall}} \quad (7\text{-}1)$$

$$Q^*_p = \varepsilon(\varphi^*\varphi_0)\frac{k_p}{k_f}\left(\frac{\partial T^*_p}{\partial y^*}\right)_{\text{wall}} \quad (7\text{-}2)$$

$$Q^*_s = (1-\varepsilon)\frac{k_s}{k_f}\left(\frac{\partial T^*_f}{\partial y^*}\right)_{\text{wall}} \quad (7\text{-}3)$$

where φ^* is the dimensinless volume fraction of particles at the channel center.

Delivered by Publishing Technology to: Guest User
IP: 31.214.93.254 On: Thu, 13 Dec 2013 21:45:22
Copyright: American Scientific Publishers

3. BOUNDARY AND INITIAL CONDITIONS

The boundary conditions are as follows

$$\text{At } y^* = 0 \text{ and } 2 \quad T^*_f = 1, \quad T^*_p = 1, \quad T^*_s = 1, \quad \varphi^* = 0, \quad u^* = 0$$
$$\text{At } x^* = 0 \quad T^*_f = 1, \quad T^*_p = 1, \quad T^*_s = 1, \quad \varphi^* = 1 \quad (8)$$

For outlet boundary, the normal gradient of properties along the outlet is zero and the values of all properties at the outlet are interpolated from the computational domain.

At the channel outlet, $x^* = 20$:

$$\frac{\partial T^*_f}{\partial x^*} = 0, \quad \frac{\partial T^*_p}{\partial x^*} = 0, \quad \frac{\partial T^*_s}{\partial x^*} = 0, \quad \frac{\partial \varphi^*}{\partial x^*} = 0 \quad (9)$$

The initial conditions, at $t^* = 0$, are:

$$T^*_f(t^*=0), \quad T^*_p(t^*=0), \quad T^*_s(t^*=0) \quad \text{and} \quad \varphi^*(t^*=0) = 1 \quad (10)$$

4. NUMERICAL METHOD

The finite difference method is used to solve the governing equations appeared in Eqs. (1)–(5). A fully- implicit method is employed to discrete the time dependant terms. It is interesting to notice that the thermophoretic parameter i.e., $\nabla T^* \cdot \nabla T^*$ is linearized by the method specified in Patankar.[30] The uniform grids are used in the computational domain. The results of grid independence test are given in Table I. In our previous research work (Maghrebi et al.[25]), the nonlinear Darcy Brinkmann Forchheimer equation is solved by the Newton-Raphson method (see: Epperson[31]). For simplicity, the Darcy Brinkmann equation is used in this study. The coupled energy and volume fraction distribution equations are solved by a line-by-line iterative procedure which sweeps the computational domain in x–y directions (Patankar[30]). The computational procedure for the solution of governing equations can be summarized as flowchart shown on the next page.

Table I. Grid study.

Grid number	Local Nusselt number
$100 * 100$	7.5418
$200 * 200$	7.5419
$300 * 300$	7.542
$400 * 400$	7.542

5. RESULTS AND DISCUSSION

When the Nield number is equal to zero, the energy equations (for the three phases) are completely decoupled and the obtained results are the same as those of the one-equation model. This case was studied previously by Maghrebi et al.[25] Moreover, to check the accuracy of the numerical solution of Eqs. (3) and (4), the fluid temperature distribution in the case of thermal-equilibrium is derived from the previous investigation of the authors (see Maghrebi et al.[25]) and inserted into the present code for $\text{Nhs} = 10^6$ and $\text{Nhp} = 10^6$. As shown in Figure 2, the solid temperature distributions and the particle temperature distribution fully overlap the fluid temperature distribution. This corresponds to the thermal equilibrium condition.

In the present paper, the numerical results are related to $\varphi_0 = 0.03$, $\gamma_p = 10$, $\gamma_s = 10$, $\text{Pr} = 1$, $\text{Re} = 150$, $\text{Da} = 1/500$, $\tau = 1$, $(1/\text{Da})(1/H^2)(dP^*/dx^*) = -2$. $\varepsilon_s = 1000$, $\varepsilon_p = 1000$.

Figure 3 shows the effects of the Lewis number on the local heat flux absorbed by the fluid, solid and the particle phases, the temperature distribution and the volume fraction distribution, respectively. As shown in this figure, the Lewis number varies in the range of 10–10^5 and the results are obtained for $N_{\text{bt}} = 0.1$ and $\text{Sc} = 500$. The heat flux absorbed by the fluid in the channel is shown in Figure 3(a). It is obvious in the main region that the heat flux remains constant and it introduces the thermally developed region inside the porous channel. The volume fraction distribution and the temperature profile are shown in Figures 3(b) and (c) in the thermally fully developed region of the channel (at $x^* = 20$). The results show that the absorbed heat flux by the fluid is decreased by increasing the Lewis number. As the Lewis equation suggests, any decrease in the Brownian diffusion coefficient (D_B) leads to an increase in the Lewis

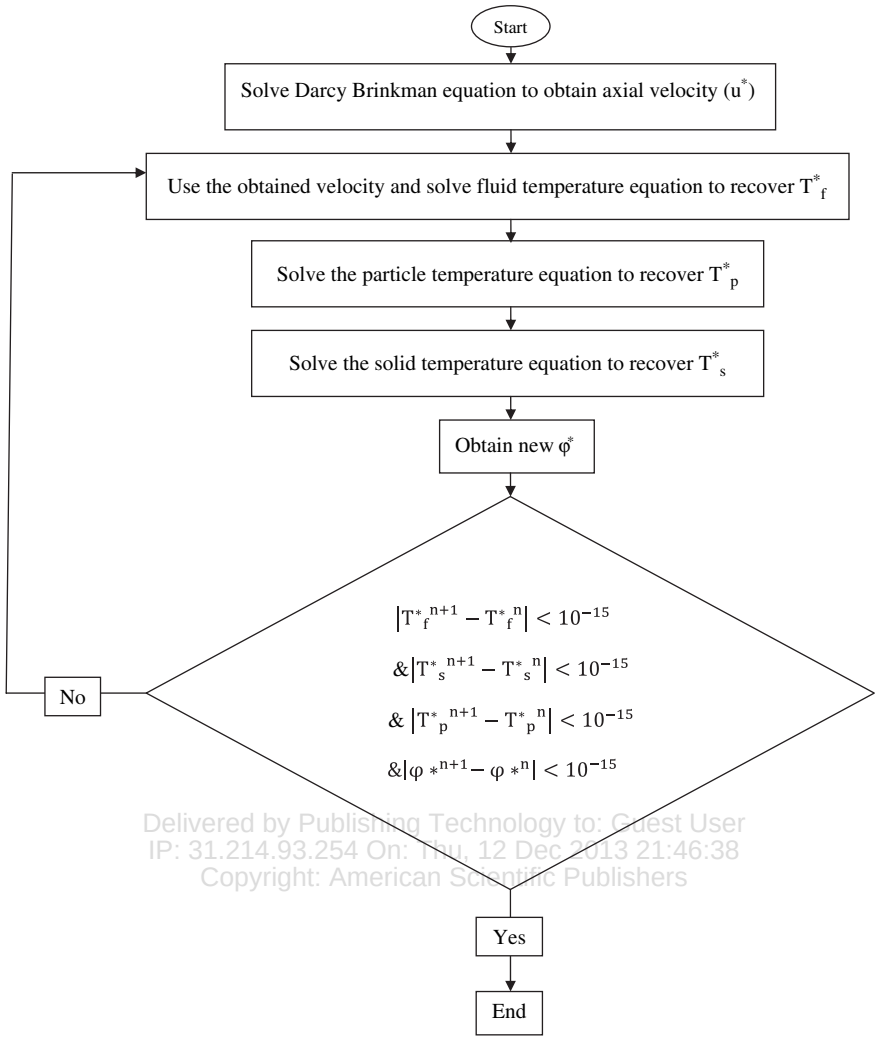

Delivered by Publishing Technology to: Guest User
IP: 31.214.93.254 On: Thu, 12 Dec 2013 21:46:38
Copyright: American Scientific Publishers

number. For preserving N_{bt} constant the denominator of its equation should decrease as D_B decreases. In other words, the thermophoretic diffusion coefficient (D_T) should be decreased to keep N_{bt} unchanged.

The volume fraction distribution doesn't have a significant effect due to a change in large Lewis number (see Fig. 3(b)). But totally at large Lewis numbers, the particles migrate to the center of the channel. The governing equations suggest that the energy equation is affected by the Lewis number. Therefore, the local absorbed heat flux by the fluid and the fluid temperature distributions are influenced by the variation of the Lewis number. The temperature gradient near the wall is decreased as the Lewis number is increased and as a result, the local absorbed heat flux decreases. For large Lewis numbers, Eq. (2) is simplified to the classical "channel-flow energy equation" without the effects of Brownian motion and thermophoresis. Because of thermophoresis and Brownian diffusion, particles migrate away from the vicinity of wall to the center of the channel. In this study, the solid temperature distribution and the particle temperature distribution are completely overlapped. That is because the Nield number and modified thermal capacity ratio for both of these equations have the same value. Figure 3(d) shows the effect of the Lewis number on the solid or particle temperature distribution. This indicates that when the Lewis number is increased, the solid temperature distribution is decreased.

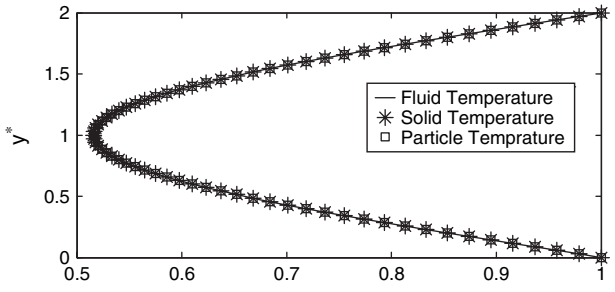

Fig. 2. Fluid temperature and solid temperature and particle temperature at Nhs = 10^6 and Nhp = 10^6.

Figures 3(e) and (f) show the heat flux absorbed by the solid and the particles, receptively. As shown by

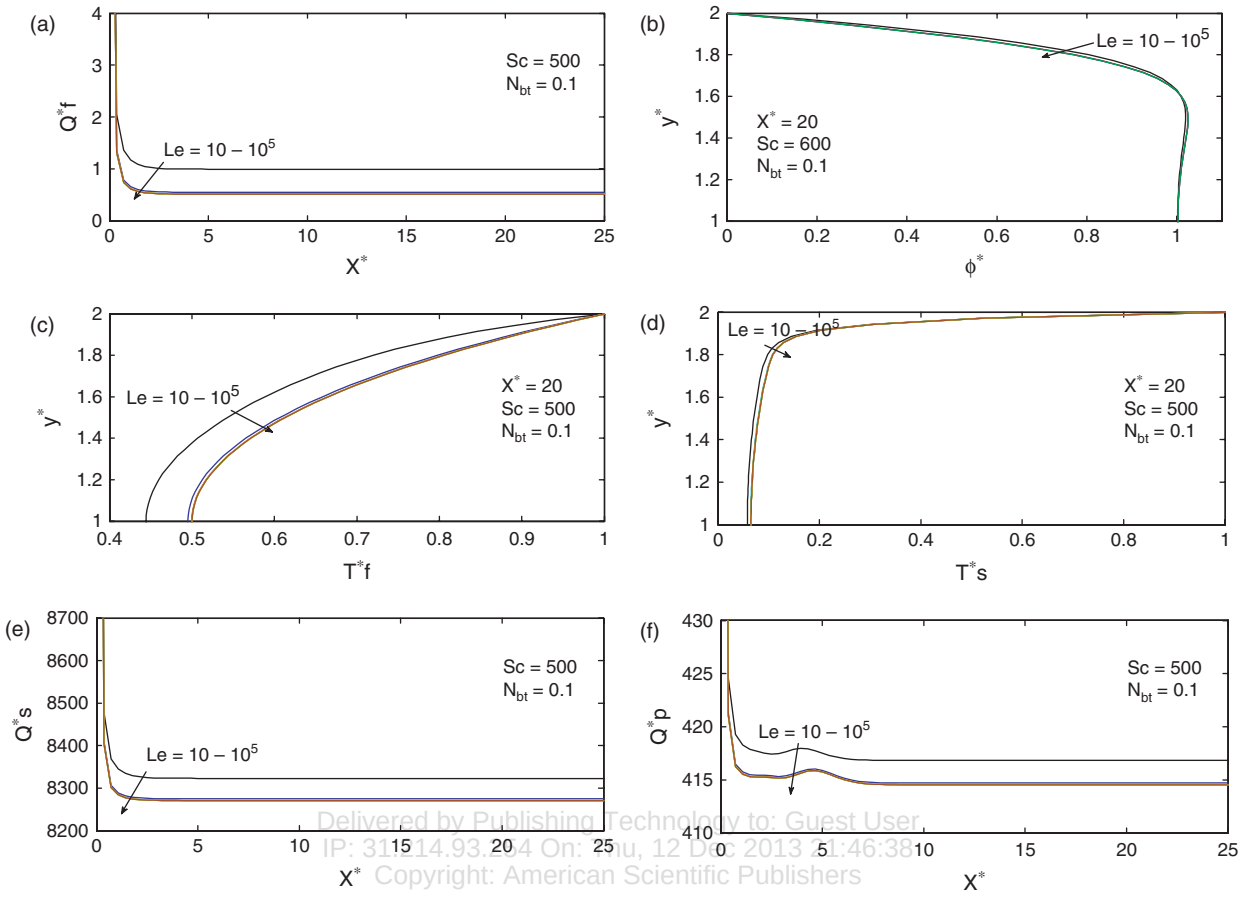

Delivered by Publishing Technology to: Guest User
IP: 31.214.93.204 On: Thu, 12 Dec 2013 21:46:38
Copyright: American Scientific Publishers

Fig. 3. (a) Heat flux absorbed by fluid various with Lewis Number (Le), (b) Volume fraction distribution various with Le, (c) Fluid temperature distribution changing via versus Le. (d) Solid/Particle temperature distribution for different Le numbers at Sc = 500 and $N_{bt} = 0.1$. (e) and (f) Heat flux absorbed by solid and particle respectively.

the results, when the Lewis number is increased, the wall temperature gradient (and hence the heat flux) is decreased. The particle heat flux is affected by the particle volume fraction at the center of the channel and the particle temperature gradient near the wall. The first parameter is increased by increasing the Lewis number and the second parameter is decreased and the dominant term then the absorbed heat flux is decreased.

Figure 4 displays the effect of N_{bt} on the fluid, solid and the particle heat fluxes, temperature distribution and the volume fraction distribution. These parameters can be expressed as the ratio of the Brownian diffusion to the thermophoresis diffusion. N_{bt} changes within the range of 0.1–0.5. The Schmidt and Lewis numbers are also set to 10 and 500, respectively. Figure 4(a) shows the volume fraction distribution for different values of N_{bt}. As the wall has the highest temperature, the particles have a tendency to migrate to the channel center. In other worlds, according to N_{bt} and Schmidt's equations for a fixed value of D_B, Lewis and Schmidt numbers, any increase in the thermophoretic parameter (D_T) results in particle migration to the center of channel. As N_{bt} equation indicates, any increase in D_T has the same effect as a decrease in N_{bt}. Therefore, any decrease in N_{bt} causes the particles to migrate to the center of the channel. Figure 4(a), shows this concept completely. A decrease in N_{bt} (i.e., increasing the thermophoretic parameter) leads to an increase in the volume fraction of particles at a specific location inside the channel. Figures 4(b) and (c) show the fluid dimensionless temperature distribution and the absorbed heat flux by fluid in the channel for different values of N_{bt}. Figure 4(c) indicates that as N_{bt} increases, the absorbed heat flux by fluid decreases. It is interesting to notice that any increase in N_{bt} leads to a decrease in the gradient of fluid temperature at the wall, and therefore, a decrease in the absorbed heat flux.

The results indicate that when the Lewis and Schmidt numbers are not very large, the absorbed heat flux and the temperature distribution change considerably. In contrast, for large values of the Lewis and Schmidt numbers, the absorbed heat flux and the temperature distribution curves do not indicate a significant change with N_{bt}. Figure 4(d) shows the effect of N_{bt} number on the solid or particle temperature distribution. It is observed that when N_{bt} number is increased, the solid temperature distribution is decreased and the particles follow the similar trend. Figures 4(e) and (f) show the heat flux absorbed by the solid and

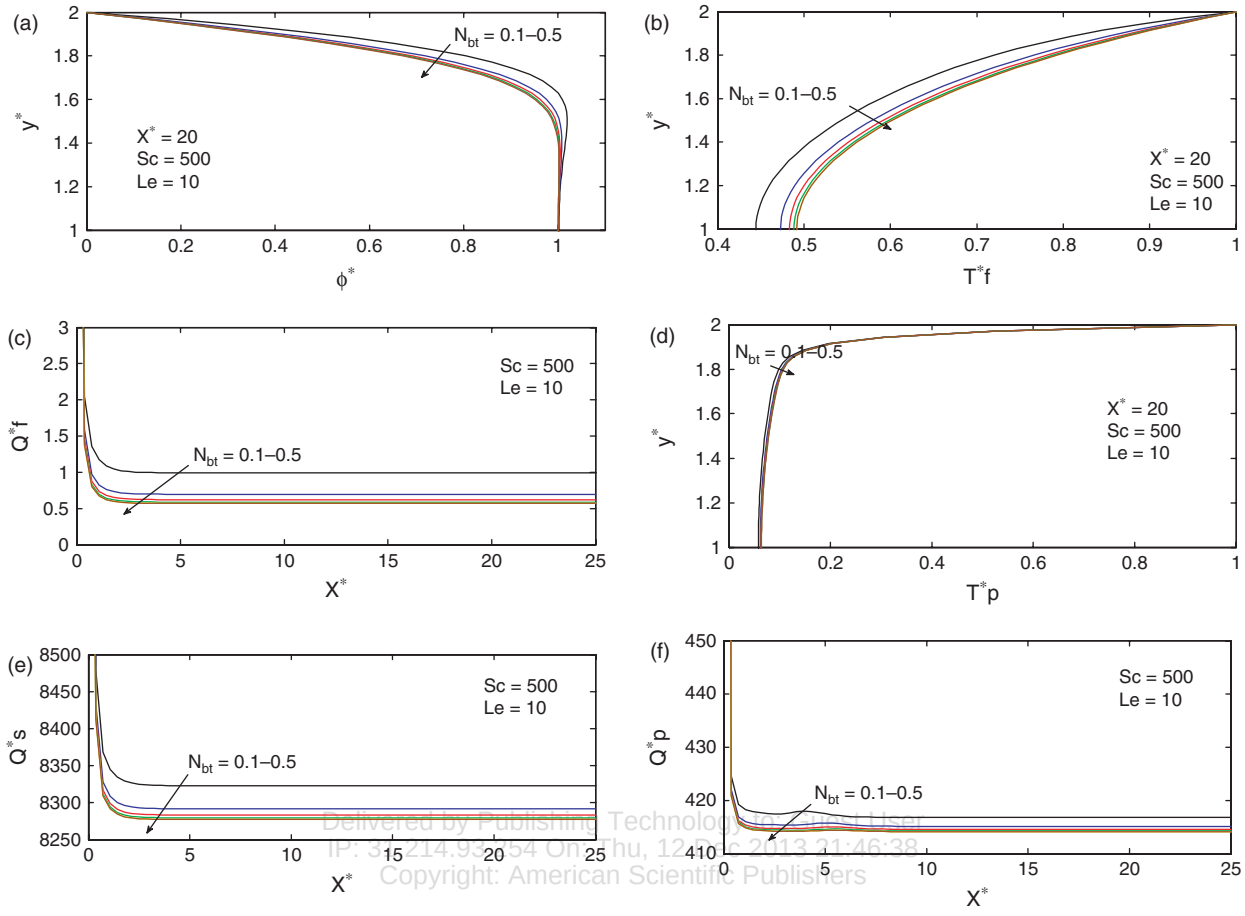

Delivered by Publishing Technology to: Guest User
IP: 3[illegible]214.93.254 On: Thu, 12 Dec 2013 21:46:38
Copyright: American Scientific Publishers

Fig. 4. (a) Volume fraction distribution for different values of N_{bt}, (b) Fluid temperature distribution versus X^* for different N_{bt} values, (c) Heat flux absorbed by fluid for different N_{bt}'s. (d) Variation of solid/particle temperature for different N_{bt} values, (e) and (f) Heat flux absorbed by solid and particle respectively.

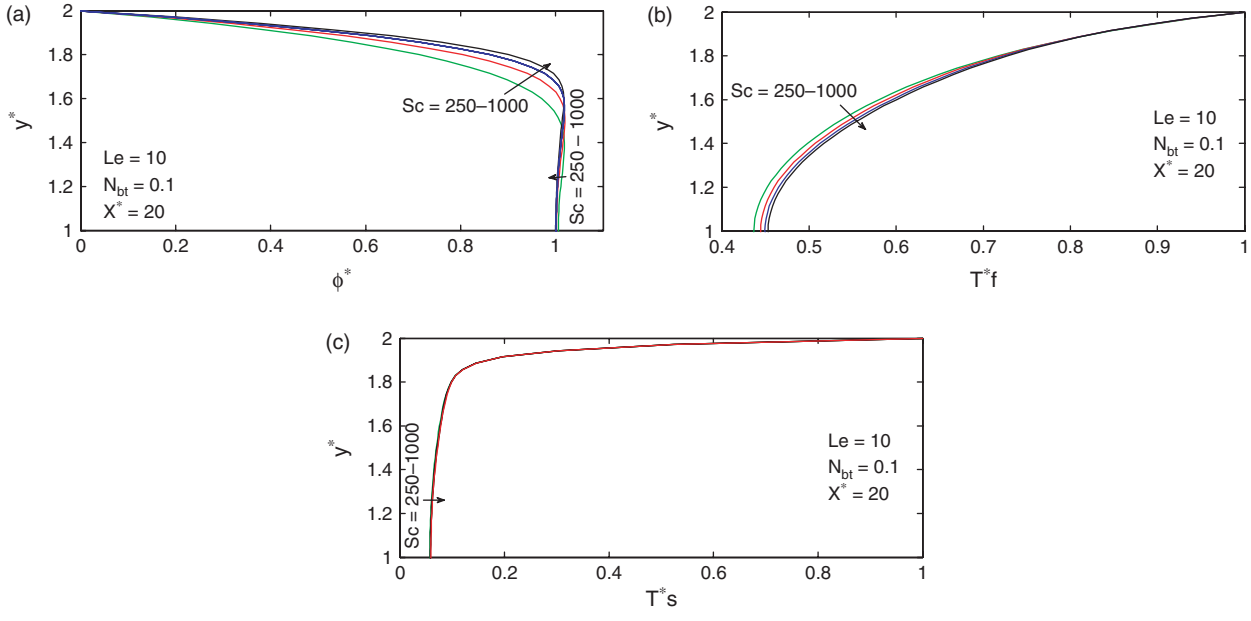

Fig. 5. (a) Variation of volume fraction distribution with Sc, (b) and (c) Fluid and solid (or particle) temperature distribution for different Sc numbers.

particle phases, respectively. When N_{bt} is increased, the wall temperature gradient for the solid and the particles are decreased and as a result, the absorbed heat flux by the solid and the particles are decreased.

Figure 5 shows the effects of the Schmidt number which varies within the range of 250–1000 on the mentioned characters. N_{bt} and Lewis number are fixed at 0.1 and 10 respectively. When the Schmidt number is increased, the right hand side of Eq. (5) is decreased so that the effects of Brownian motion and thermophoresis are vanished. Figure 5(a) shows the volume fraction distribution versus the Schmidt number. As the figure shows at a large Schmidt number, the convective term is dominant and the volume fraction distribution inside the channel behaves similar to the inlet volume fraction distribution. Figure 5(b) shows the temperature distribution in the channel. Figure 5(c) shows the effect of the Schmidt number on the solid or the particle temperature distribution. It seen from the results that when the Schmidt number is increased, the solid temperature distribution is decreased and the particle follow the same trend. The heat flux absorbed by the fluid, solid and the particles does not show any significant change with the Schmidt number.

6. CONCLUSIONS

This paper was concerned with the effects of flow and migration of nanoparticles on heat transfer in a straight channel occupied with a porous medium. The fully-developed flow and steady Darcy-Brinkman equation was employed in the porous channel. The local thermal non-equilibrium model was assumed between the pure fluid, solid and the nanoparticle phases. It was assumed that the nanoparticles are distributed non-uniformly inside the channel. The effects of the Lewis number, Schmidt number and the modified diffusivity ratio (N_{bt}) on the heat transfer were completely studied. The results showed that the non-dimensional heat flux absorbed by the fluid decreased when the Lewis number was increased. This behaviour was also observed in the heat flux absorbed by the particles and the solid. The effects of the Schmidt number, Lewis number and N_{bt} on the volume fraction distribution and heat flux were also studied numerically. The results indicated that when the Schmidt number was increased, the particle distribution tended to the entrance distribution.

Delivered by Ingenta to: Technology & Health User
IP: 31.24.92.254 On: Thu, 12 Feb 2015 ...
Copyright: American Scientific Publishers

NOMENCLATURE

xy Cartesian coordinate (m)
u Axial velocity (ms^{-1})
K Permeability (m^2)
Da Darcy number
P Pressure (Nm^{-2})
T Temperature (K)
D_T Thermophoretic diffusion coefficient ($\mathrm{m}^2\ \mathrm{s}^{-1}$)
D_B Brownian diffusion coefficient ($\mathrm{m}^2\ \mathrm{s}^{-1}$)
H Half length of channel
t Time(s)
Re Reynolds number
Pr Prantdl number
N_{BT} Brownian motion parameter
k Thermal conductivity ($\mathrm{wm}^{-1}\ \mathrm{K}^{-1}$)
Le Lewis number
Sc Schmitt number
N_{HP} Nield number for the fluid/particle interface
h_{fs} Heat transfer coefficient between the fluid/solid.
N_{HS} Nield number for the fluid/solid matrix interface
h_{fp} Heat transfer coefficient between the fluid/particle.

Greek Letters

μ Viscosity ($\mathrm{kgm}^{-1}\mathrm{s}^{-1}$)
ε Porosity
ρ Density (kgm^{-3})
φ Volume fraction
σ Thermal capacity ratio
ε_p Modified thermal diffusivity ratio by $\varepsilon_p = (k_p/k_f)\cdot((\rho c)_f/(\rho c)_p)$
ε_s Modified thermal diffusivity ratio by $\varepsilon_s = (k_s/k_f)\cdot((\rho c)_f/(\rho c)_s)$
γ_p Modified thermal capacity ratio by $\gamma_p = ((1-\varphi_0)/\varphi_0)((\rho c)_f/(\rho c)_p)$
γ_s Modified thermal capacity ratio by $\gamma_s = (\varepsilon(1-\varphi_0)/(1-\varepsilon))((\rho c)_f/(\rho c)_s)$
α Effective thermal diffusivity ($\mathrm{m}^2\mathrm{s}^{-1}$)
τ Modified diffusivity ratio.

Subscript

s solid
f fluid
p particle
$*$ Dimensionless variables

References and Notes

1. S. U. S. Choi, *Devel. Appl. Non-Newtonian Flows* 66, 99 **(1995)**.
2. W. Duangthongsuk and S. Wongwises, *Int. J. Heat and Mass Transf.* 52, 2059 **(2009)**.
3. A. K. Santra, S. Sen, and M. Chkroborty, *Int. J. Therm. Sci.* 48, 391 **(2009)**.
4. C. T. Nguyen, N. Galanis, G. Polidori, S. Fohanno, C. V. Pota, and A. L. Beche, *Int. J. Therm. Sci.* 48, 401 **(2009)**.
5. M. H. Kayhani, M. Nazari, H. Soltanzadeh, M. M. Heyhat, and F. Kowsary, *Micro and Nano Lett.* 7, 223 **(2012)**.
6. M. H. Kayhani, H. Soltanzadeh, M. M. Heyhat, M. Nazari, and F. Kowsary, *Int. Comm. Heat and Mass transf.* 39, 456 **(2012)**.
7. X. Q. Wang and A. S. Mujumdar, *Int. J. Therm. Sci.* 46, 1 **(2007)**.
8. A. Behzadmehr, M. Saffar-Avval, and N. Galanis, *Int. J. Heat Fluid Flow* 28, 211 **(2003)**.
9. M. J. Maghrebi, T. Armaghani, and F. Talebi, *Therm. Scie. J.* 16, 455 **(2012)**.
10. J. Lee and I. Mudawar, *Int. J. Heat and Mass Transf.* 50, 452 **(2007)**.
11. T. Tayebi, M. Djezzar, and K. saadaoui, *J. Nanofluids* 2, 120 **(2013)**.
12. J. Buongiorno, *ASME J. Heat Transf.* 128, 240 **(2006)**.
13. M. M. Heyhat and F. Kowsary, *ASME J. Heat transf.* 132, 062401 **(2010)**.
14. A. V. Kuznetsov and D. A. Nield, *Trans. Porous Media* 81, 409 **(2010)**.

15. A. V. Kuznetsov and D. A. Nield, *Trans. Porous Media* 83, 425 **(2010)**.
16. A. V. Kuznetsov and D. A. Nield, *J. Porous Media* 14,285 **(2011)**.
17. D. A. Nield and A. V. Kuznetsov, *Int. J. Heat and Mass Transf.* 54, 374 **(2011)**.
18. A. V. Kuznetsov and D. A. Nield, *Int. J. Therm. Sci.* 50, 712 **(2011)**.
19. M. Hajipour and A. M. Dehkordi, *Int. J. Therm. Sci.* 55, 103 **(2012)**.
20. N. Prabhat, J. Buongiorno, and L.-W. Hu, *J. Nanofluids* 1, 55 **(2012)**.
21. G. H. Li, P. Jiang, and G. P. Peterson, *J. Nanofluid* 2, 20 **(2013)**.
22. W. Yu, D. M. France, E. V. Timofeera, and D. Singh, *J. Nanofluids*, 2, 69 **(2013)**.
23. A. Mahajan, M. Arora, and Sunil, *J. Nanofluids* 2, 147 **(2013)**.
24. R. S. R. Gorla and M. Kumari, *J. Nanofluids* 1, 186 **(2012)**.
25. M. J. Maghrebi, M. Nazari, and T. Armaghani, *Transp. Porous Media* 93, 401 **(2012)**.
26. D. A. Nield, A. V. Kuznetsov, and M. Xiong, *Int. J. Heat and Mass Transf.* 46, 643 **(2003)**.
27. P. Vadasz, *ASME J. Heat Transf.* 128, 465 **(2006)**.
28. D. A. Niled, *J. Porous Media,* 1, 181 **(1998)**.
29. A. Amiri, K. Vafai, and T. M. Kuzay, *Numer. Heat Transf, Part A* 27, 651 **(1995)**.
30. S. V. Patankar, Numerical Heat Transfer and Fluid Flow, Hemisphere, New York **(1980)**.
31. J. F. Epperson, An Introduction to Numerical Methods and Analysis, John Wiley & Sons **(2010)**.

Delivered by Publishing Technology to: Guest User
IP: 31.214.93.254 On: Thu, 12 Dec 2013 21:46:38
Copyright: American Scientific Publishers